Chapter 4
Aluminates

Martin C. Wilding

Abstract Aluminates form in binary systems with alkali, alkaline earth or rare-earth oxides and share the high melting point and resistance to chemical attack of the pure Al_2O_3 end-member. This means that these ceramics have a variety of applications as cements, castable ceramics, bioceramics, and electroceramics. Calcium aluminate cements are used for example in specialist applications as diverse as lining sewers and as dental restoratives.

Ceramics in aluminate systems are usually formed from cubic crystal systems and this includes spinel and garnet. Rare earth aluminate garnets include the phase YAG (yttrium aluminium garnet), which is an important laser host when doped with Nd(III) and more recently Yb(III). Associated applications include applications as scintillators and phosphors.

Aluminate glasses are transparent in the infrared region and these too have specialist applications, although the glass-forming ability is poor. Recently, rare earth aluminate glasses have been developed commercially in optical applications as alternatives to sapphire for use in, for example, infrared windows.

Aluminates are refractory materials and their synthesis often simply involves solid-state growth of mixtures of purified oxides. Alternative synthesis routes are also used in specialist applications, for example in production of materials with controlled porosity and these invariably involve sol–gel methods. For glasses, one notable, commercially important method of production is container-less synthesis, which is necessary because of the non-Arrhenius (fragile) viscosity of aluminate liquids.

1 Introduction

Glasses and ceramics based on the Al_2O_3-based systems have important applications as ceramic materials, optical materials, and biomedical materials. Aluminate materials include alkaline earth aluminates, such as those in the $CaO–Al_2O_3$ system, which are refractory cousins of hydrous Portland cement [1–3]. Calcium aluminates have a role as both traditional ceramic and cement materials and are used for example as refractory cements; however, calcium aluminates are also important for more novel applications

J.F. Shackelford and R.H. Doremus (eds.), *Ceramic and Glass Materials: Structure, Properties and Processing*.

such as bioceramics [4–8]. Rare earth (yttrium and the lanthanides) aluminates are important laser host materials. Yttrium aluminum garnet (YAG) is one of the most common laser hosts; Nd-doped YAG lasers with powers of up to 5 kW are important for welding and cutting applications and have the further advantage of being solid state, the primary laser component being a single crystal of Nd-doped YAG. Associated with the laser properties of YAG are the materials characteristics of rare earth aluminates, which favor applications as refractory ceramics, composite laser hosts, and glass fibers that are important for optical applications, but also can be used in composite materials [9, 10].

Many of the important desirable properties that make aluminates important in materials science are similar to those of the end-member Al_2O_3. This includes the refractory nature of aluminates, for example Al_2O_3 melts at 2,054°C and other important aluminates have similarly high melting points (Table 1). In addition, aluminates have high hardness, high strength, and are resistant to chemical attack. Al_2O_3 and both calcium and rare earth aluminate systems can have useful properties such as transparency in the infrared region, and this makes aluminate glasses important for use as optical fibers. Because of their optical applications, aluminate glasses have been studied extensively and as a consequence some very unusual and anomalous thermodynamic properties have come to light.

The refractory nature of aluminates means that high temperature synthesis techniques are required. Depending on the application, aluminates can be made by mixing of oxides and subjecting the mixtures to high temperature, as for example in the manufacture of cement. For other applications, such as optical uses, more exotic techniques are used. These include high temperature melting, single crystal growth [11, 12], container-less synthesis of glasses using levitation [13], and low-temperature routes such as sol–gel synthesis [14, 15] and calcining.

There are a variety of important crystal structures in aluminate systems. Among the most important are the spinel [16] and garnet structures [17, 18]. These various structures reflect differences in the coordination polyhedron of both Al(III) and added components such as Mg(II), Ca(II), and the rare earth ions. In addition, studies of glass structure suggest a wealth of different coordination environments for both Al(III) and added components and structures that are not simply disordered forms of crystalline phases.

For the purposes of this review, aluminates can be defined as a binary section of a ternary oxide system with Al_2O_3 as one component. A large number of different aluminates can be made and it is not the purpose of this chapter to provide an exhaustive list of each different aluminate type or each application. Rather, it is the purpose of this chapter to provide a survey of the range of binary Al_2O_3-systems and to demonstrate the diversity of both their applications to materials science and to elaborate on the unusual

Table 1 The physical properties of selected binary aluminate ceramics

	Melting temperature (K)	Density (g cm^{-3})	Hardness (Knoop/100 g) (Kg mm^{-2})	Compressive strength (MPa)	Tensile strength (MPa)	Young's modulus (GPa)
α-Al_2O_3	2,327	3.98	2,000–2,050	2,549	255	393
$CaAl_2O_4$	2,143	2.98				
$MgAl_2O_4$	2,408	3.65	1,175–1,380	1,611	129	271
$LiAlO_2$	1,883	2.55			350	
$Y_3Al_5O_{12}$	2,243	4.55	1,315–1,385		280	282

structural and thermodynamic properties of crystalline and glassy aluminate materials. Three subsets of aluminates will be highlighted: binary alkaline earth aluminates (CaO, $MgO–Al_2O_3$), which includes calcium aluminate cements and magnesium aluminate spinels, alkali (lithium) aluminates, which potentially have very important applications in the development of new types of nuclear reactors [19], and rare earth aluminates, particularly compositions close to that of the yttrium aluminum garnet ($Y_3Al_5O_{12}$; YAG). Each section will discuss the applications, structure, and synthesis of each composition, and finally the thermodynamic and structural properties of these aluminates will be compared and summarized.

2 Alkali and Alkaline Earth Aluminates

There are two important systems discussed in this section: $CaO–Al_2O_3$ and $MgO–Al_2O_3$. In addition, there are sometimes other binary systems and mixtures or small amounts of additional elements added to the binary systems such as SrO, added to improve glass forming ability [20, 21]. For convenience, these latter more complex systems will be discussed with the strict binary $CaO–Al_2O_3$ phases.

3 Calcium Aluminate Cements

Calcium aluminate phases are used as cements in refractory and other specialized applications [1, 2, 22, 23]. The ceramics in the calcium aluminate ($CaO–Al_2O_3$) system are closely related to Portland cements and have similar properties in terms of rapid hardening and setting times [24]. Their phase equilibria are closely related to that of Portland cements as and are formed in the binary $CaO–Al_2O_3$ of the ternary $CaO–Al_2O_3–SiO_2$ phase diagram. The binary phase diagram (Fig. 1) shows that calcium aluminate cements (CACs) have a wider range of compositions than Portland cements, but are dominated by the monocalcium aluminate ($CaAl_2O_4$, also referred to as CA).

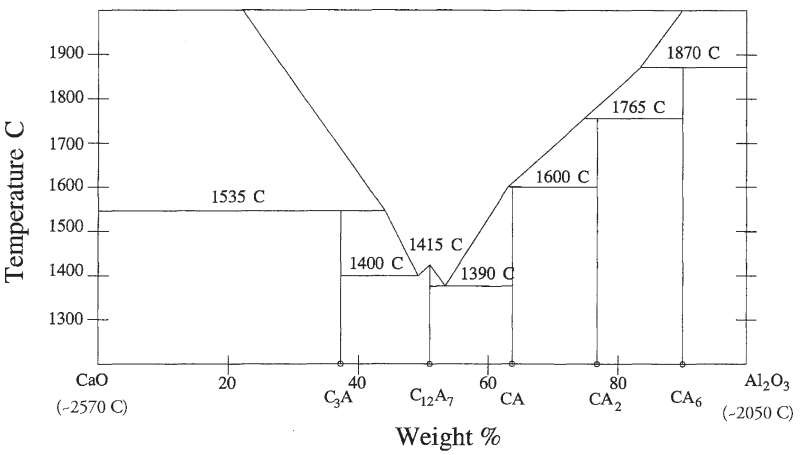

Fig. 1 The $CaO–Al_2O_3$ phase diagram [25, 26]

CACs were developed in response to the need for cements resistant to groundwater and seawater attack and are the only cements, other than Portland cement, that are in continuous long-term production [2]. The property of CAC that was most important in their commercial development is the resistance to sulfate attack, which contrasted with the poor-sulfate resistance of contemporary Portland cements [2], and CAC was first patented in 1908 [2]. Most early applications, in construction projects following the First World War, were in structures exposed to seawater, such as harbor pilings. Because CAC hardens rapidly, it was adopted for prestressed concrete beams in the post World War II construction boom, with some unfortunate results. Poor understanding of the material properties of CAC and incorrect water to cement ratios led to the collapse of several buildings, and the use of Portland cements, which are cheaper, has replaced CAC in prestressed concrete beams[2].

There are, however, several important niche applications for CAC. Most notably, CACs are used as linings to sewers and mine tunnels. Calcium aluminate cements are resistant to chemical attack from sulfate-producing bacteria that thrive in sewer systems (especially in warmer climates), and sprayed concrete linings to sewers have been shown to resist degradation for periods up to 30 years. The high impact and abrasion resistance of CAC also makes it suitable as a lining material for ore tunnels in mines and because CAC sets rapidly, it can be sprayed onto tunnel walls (as "shotcrete") and even used as a tunnel lining.

Additional specialist applications include castable refractory ceramics and use as bioceramics, which are discussed later.

4 Phase Equilibria and Crystal Phases in the $CaO–Al_2O_3$ System

The binary phase diagram of $CaO–Al_2O_3$ shows two refractory end-members CaO and Al_2O_3 with melting points of 2,570°C and 2,050°C, respectively [25, 26]. There is a deep eutectic with a minimum at 1,390°C and five intermediate crystalline phases, of which three hydrates are important as cements [27].

Monocalcium aluminate ($CaAl_2O_4$) is the most important phase in CAC. Addition of water to $CaAl_2O_4$ (CA) eventually leads to the formation of the crystalline hydrates $3CaO{\cdot}Al_2O_3{\cdot}6H_2O$ and $Al_2O_3{\cdot}3H_2O$, which dominate the initial hydration of CAC [27]. Monocalcium aluminate $CaAl_2O_4$ does not have a spinel structure, even though it is stochiometrically equivalent to Mg-aluminate spinel. The crystal structure of this phase is monoclinic, pseudo hexagonal with a p2/n space group. The structure of the CA phase resembles that of tridymite and is formed from a framework of corner-linked AlO_4 tetrahedra. Large Ca^{2+} ions distort the aluminate framework, reducing symmetry. As a consequence, the coordination environment of Ca^{2+} is irregular.

The CA2 phase ($CaO{\cdot}2Al_2O_3$) occurs as the natural mineral grossite [27]. This phase is a monoclinic C2/2 phase and is also formed from a framework of corner-linked AlO_4 tetrahedra. Some of the oxygens in the framework are shared between two tetrahedral and some are shared between three. The CA2 phase does not react well with H_2O and is not necessarily useful in refractory CAC. The CA6 phase also occurs naturally, as the mineral hibenite. This phase has a similar structure to β-Al_2O_3 and is nonreactive and its presence is not desired in CAC.

The C12A7 phase reacts very rapidly with water and becomes modified to produce the hydrated phase $11CaO{\cdot}7Al_2O_3{\cdot}Ca(OH)_2$. The C12A7 phase is cubic with a space group of 143 d. The basic structure is one of a corner shared AlO_4 framework. The Ca^{2+} ions are coordinated by six oxygen atoms but the coordination polyhedron is irregular. It has been suggested, by infrared spectroscopy, that some of the aluminum ions are coordinated by five oxygen atoms. This hydrated phase ($Ca_{11}Al_7{\cdot}Ca(OH)_2$) is closely related to the naturally occurring mineral, Mayenite, a cubic mineral with M2M symmetry and a large (11.97 Å) unit cell, closely related to the garnet structure.

5 Refractory Castables

One very important niche application for calcium aluminate (cements) is as refractory castables. Key to the success of calcium aluminates in this application are their refractory properties that contrast with those of Portland cements. Although Portland cement maintains good strength when heated, reactive components (CaO) are liberated and can absorb moisture from the atmosphere when cooled, causing expansion and deterioration of, for example, kiln linings. CACs are not much susceptible and can be used to form monolithic castables and refractory cements [28, 29].

6 Calcium Aluminate Bioceramics

Ceramic materials with high strength, high wear resistance, and high resistance to corrosion can be used as prosthetic replacements for bones and teeth. One important consideration for potential bioceramics is compatibility with the human body, since for example hip prostheses are placed in vivo. Bones and teeth comprise hydroxyapatite, a calcium bearing phase and Ca^{2+} ions are mobile during formation. Calcium aluminates are attractive for bioceramic applications; because of the mobility of Ca^{2+} in biological fluids these cements can bond to bone and are quick setting and during hardening form enough hydrates to fill the initial porosity and result in a high strength end-product. In addition, for dental applications CAC have similar thermal properties to teeth and are translucent, therefore even on the basis of aesthetic appearance are useful as a dental restorative [5–8, 30, 31].

7 Synthesis of Calcium Aluminates

CAC require large industrial facilities, similar to those used to make ordinary Portland cement. The raw materials for CAC are typically bauxite and limestone, which are ball-milled and mixed together to form a feed of appropriate composition, which is fed into rotary kilns to form a calcium aluminate clinker. The clinker is ball-milled to produce the cement. Analysis for composition and mineralogy at various stages of manufacture are essential to ensure a consistent product, see for example Chakraborty and Chattopadhyay [32] for a discussion of the bulk processing of high alumina CAC.

For high purity calcium aluminate compositions, solid-state synthesis is still the norm [33, 34]. Most CAC compounds are made by solid-state reactions between ground powders of calcium carbonate and purified alumina. The sintering temperatures depend on alumina content. More recently attempts have been made to synthesize CA compounds using processes with temperatures less than 900°C. These latter methods include sol–gel synthesis and precipitation and are important for production of high-purity homogenous powders with small grain size.

Amorphous calcium aluminate powders have been synthesized chemically by Uberoi and Risbud [35] by sol–gel methods. These materials were made from calcium nitrate ($Ca(NO_3)_2$) and by using aluminum di-sec-butoxide acetoacetic ester chelate ($Al(OC_4H_9)_2(C_6H_9O_3)$) as the source of alumina.

A further synthesis method is self-propagating combustion synthesis [33, 36, 37]. In this alternative approach, nitrate starting powders are dissolved in H_2O and urea (CH_4N_2O) is added. When this mixture is boiled, dehydrated, and dried, it forms a hygroscopic precursor to calcium aluminates, which can be crystallized by heating in dry air between 250 and 1,050°C. The gaseous decomposition products of the precursor mixture are NH_4 and HCNO, which ignite at ~500°C, locally the temperature in the dried foam increases to ~1,300°C, which promotes crystallization of the CAC phase.

8 Calcium Aluminate Glasses

Calcium aluminate glasses have the potential for a variety of mechanical and optical applications; [20, 21, 38–46] however, they are difficult to form. Addition of SiO_2 can be used to improve glass-forming ability, although this reduces the optical properties, particularly the transparency to infrared, so it is best avoided. Studies show that the best glass-forming composition in the $CaO–Al_2O_3$ binary is close to the composition $64CaO–36Al_2O_3$ [45].

Calcium aluminate glasses form from “fragile” liquids [47], and these deviate from an Arrhenius viscosity–temperature relation. Because of these distinct rheological properties, calcium aluminate glasses have been extensively studied by diffraction and spectroscopic techniques. The composition-dependence of calcium aluminate structures was studied by McMillan for almost the entire range of $CaO–Al_2O_3$ liquids [45] using extremely rapid quench techniques. Extensive NMR and Raman data obtained from these rapidly quenched glasses show a range in Al–O coordination. For $CaO/Al_2O_3 < 1$, the glasses are dominated by $^{[IV]}$Al. NMR and Raman data indicate that there are changes in mid-range order and also in relaxation time (i.e., viscosity), as expected for fragile liquids [45]. The changes in Raman and NMR spectra are interpreted as different degrees of distortion of the Al–O coordination polyhedron as the identity of next-nearest neighbor changes. Raman data support this interpretation, in that there is no evidence for change in AlO_4 polymerization. Similarly, X-ray absorption spectroscopy shows dramatic changes in spectra with quench rate, and changes in next-nearest neighbor. For calcium aluminates it is argued that the rearrangement of next-nearest neighbors reflects over- and under-bonding of the central ion in the Al–O coordination polyhedron, dependent on the degree of distortion.

Neutron and combined neutron and X-ray diffraction data for 64:36 and 50:50 calcium aluminate glasses [40, 48] have been used to determine Al–O and Ca–O coordination

environments and mid-range order changes. These studies show that the Al–O correlation at 0.176 nm and the area below this peak yield a first-neighbor coordination number of 4.8. There is a peak in the pair-correlation function at 0.234 nm, which corresponds to Ca–O; the area beneath this peak yields a coordination number of 4.0, inconstant with the value obtained from the radial distance by bond–valence theory [48]. Further examination of the diffraction data reveals a second Ca–O distance at 0.245 nm. Combined diffraction data suggest that the Ca–O polyhedron is quite distorted [40] and that the glass consists of a corner-shared Al–O framework with the Al–O units corner- and edge-shared with distorted Ca–O polyhedra.

9 Synthesis of Calcium Aluminate Glasses

Calcium aluminate glasses can be made using a variety of techniques, depending on the composition required. The ease of devitification is a considerable concern if calcium aluminate glasses are to be used for optical purposes. Although a strong network former such as SiO_2 can be added to improve glass-forming ability, this has detrimental effects on the optical properties.

Calcium aluminate glasses can be made quite easily by air quenching liquids of 61:39 composition, which is the composition most extensively used for glass fiber production [20, 44]. The glass-forming ability is considerably enhanced by adding components such as BaO, SrO, and NaO [21] without affecting the optical performance.

A further method of glass synthesis is container-less levitation techniques [39, 40, 49]. In this method, a ceramic precursor of appropriate composition is levitated by a gas jet and laser heated. Samples up to 4-mm diameter can be levitated in this way and because there is no container, heterogeneous nucleation is avoided. This means that liquids can be supercooled considerably and glasses formed from compositions are generally considered to be poor glass-formers, this includes calcium aluminate glasses. Fibers can be extracted from the levitated bead by using a tungsten "stinger" [13].

10 $MgO–Al_2O_3$ Aluminates

Magnesium aluminate phases have high melting points and like calcium aluminates are used in refractory ceramic applications. These applications include the linings of ladles in steel plants and linings for cement kilns. In these applications, ceramics are used either in the form of castables, in case of linings to labels, or as bricks (kiln linings) [50–57]. Having low phonon energy and good mechanical properties, magnesium aluminates are also emerging as an infrared window material [20].

The only stable compound in the $MgO–Al_2O_3$ system [58, 59] is spinel [16, 60] ($MgAl_2O_4$), which has a melting point of 2,105°C and in addition to being a refractory compound has high resistance to chemical attack and radiation damage [56, 61–64]. Spinel ceramics have potential use for a variety of applications in the nuclear industry because of their high resistance to radiation and are candidates for potential ceramic waste host [65–68] and have also been suggested for use within new types of nuclear reactors. Ceramic-glass composites made from Mg–Al spinels and borosilicate glass can be used for ceramic boards for large scale integrated circuits used at high temperatures [69].

The presence of Al(III) ions is believed to inhibit formation of the SiO_2 polymorph cristobalite, which degrades the mechanical and electrical properties of these specialized ceramics. Glass-spinel ceramics have the chemical and thermal resistance usually associated with aluminates and also low thermal expansion and a low dielectric constant. If there is formation of cristobalite in these types of composites, then the thermal expansion can be uneven. Temperature-dependent formation of additional SiO_2 polymorphs can lead to micro-fracturing and mechanical degradation. Decreased ceramic contents of composites improve signal transfer by further lowering of the dielectric constant and so ideally the material will have a balance of spinel and glass optimized for the improved electrical properties and minimal cristobalite formation.

11 $MgO–Al_2O_3$ System

The binary phase diagram for $MgO–Al_2O_3$ is simpler than that for the $CaO–Al_2O_3$ system (Fig. 2). There is only one stable intermediate compound that of the spinel phase (Mg_2AlO_4) [60]. Spinel melts at 2,105°C, but there is a eutectic at 1,995°C and a limited solid solution between stoichiometric spinel and MgO (periclase), up to 6 wt% MgO, can be dissolved into the spinel structure without exsolution. This limited solid solution is an important property that is utilized in manufacture of spinels for use in reducing conditions [70].

The cubic spinel crystal structure (Fd3m) is a close-packed array of oxygen ions, which has the general form AB_2O_4. A is a divalent cation and B trivalent [60, 71].

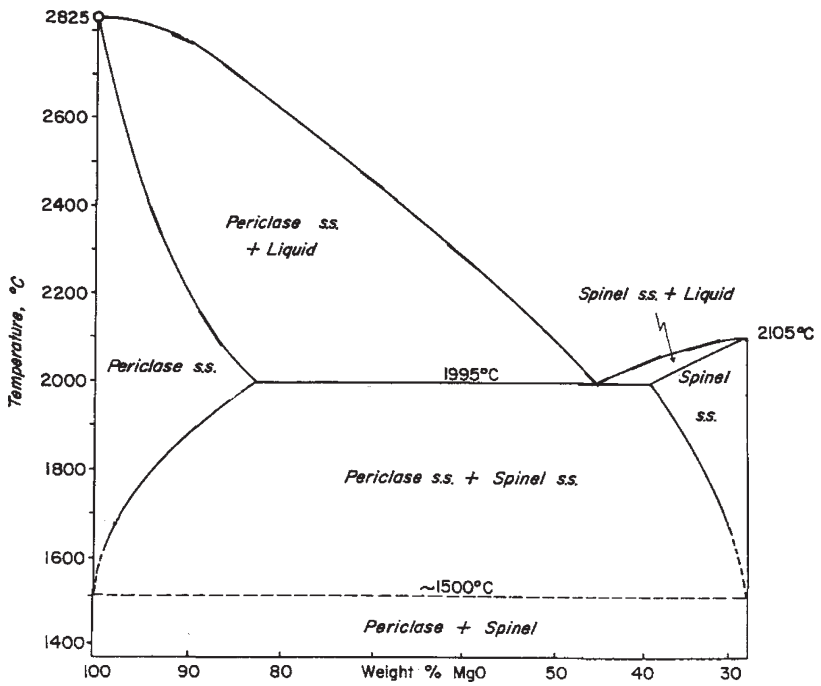

Fig. 2 The $MgO–Al_2O_3$ phase diagram [59]

The metal cations occupy two sites: divalent cations (A) are in tetrahedral coordination, while trivalent ions (B) occupy octahedral sites. The oxygen ions form a face-centered cubic close-packed arrangement and the unit cell consists of 32 oxygen ions, 8 divalent (A), and 16 trivalent ions (B) with dimensions of 0.80832 nm. There are a large number of natural forms of spinel structure, which include Cr_2O_3 and Fe_2O_3 forms. The lattice parameter A_o is 0.80832 nm, and in synthetic spinels, the limited solid solutions with both Al_2O_3 and MgO end-members are accommodated in this cubic structure, although there is slight increase in the lattice parameter [16].

There are two types of spinel, normal and inverted. Normal spinels have all the A ions in tetrahedral sites and all B ions in octahedral coordination. When the structures are inverted, the divalent A ions and half of the trivalent B ions are in the octahedral sites while the remaining B ions have tetrahedral coordination. Both normal and inverted spinels have the same cubic structure (space group Fd3m).

In high radiation fields, the spinel crystal structure has been shown to change. The structure, while still cubic, becomes disordered with a reduction in lattice parameter. The disordered "rock-salt" structure has a smaller unit cell reflecting the more random occupation of the octahedral sites by both trivalent and divalent ions. Increased radiation damage results in the formation of completely amorphous spinels. Radial distribution functions ($g(r)$) of these amorphous phases have Al–O and Mg–O radial distances that are different from equivalent crystalline phases. The Al–O distance in the amorphous form is reduced from Al–O of 0.194 nm in the crystalline phase to 0.18 nm in the amorphous phase, while the Mg–O distance is increased (0.19 nm in the crystal to 0.21 nm in the amorphous phase). Differences between the Al–O distances of crystalline and amorphous phases are a characteristic of both calcium and rare earth aluminates.

The MgO–Cr_2O_3 binary is closely related to the equivalent Al_2O_3 system. Here too the only stable compound is a spinel-structured phase $MgCr_2O_4$, which has a high melting point (2,350°C). The chrome-bearing ceramics have similar applications but have a significant drawback environmentally. There is a risk that chrome-bearing ceramics in furnace waste will interact and contaminate ground water. Cr[VI] ions leached from remnant refractory materials in wastes into ground water are a serious contaminant and have been linked to skin ulceration and carcinoma. MgO–Al_2O_3 ceramics are, therefore, much more desirable.

12 Synthesis of Magnesium Aluminates

As with many ceramics, $MgAl_2O_4$ spinels can be made by solid-state sintering of the component oxides MgO and Al_2O_3 [72]. Pure stoichiometric spinel ($MgAl_2O_4$) is made by solid-state reaction of high purity end-members at high temperatures. Starting materials are either oxides (Al_2O_3 and MgO) or carbonates ($MgCO_3$). The synthesis relies on solid-state reactions between the grains of starting material and so depends on the fineness of the powders used. An additional problem is the potential for Mg(II) to volatilize at high temperatures from the Mg-starting powder, which can lead to nonstoichiometric phases. In some instances this is desired, since more Al_2O_3-rich spinels are more stable under reducing atmospheres.

For some applications, better control on porosity is required and alternatives to solid-state synthesis methods have been sought requiring synthesis temperatures much lower than those used for the sintering route (1,600–1,800°C).

Chemical synthesis of $MgAl_2O_4$ spinels has been attempted using gibbsite ($Al(OH)_3$) and MgO precursors[73]. Spinel precursors are formed by coprecipitation and the resultant material is then calcined to produce spinel. The starting material gibbsite, which is a by-product of the Bayer process, is dissolved in a solution of HCl and HNO_3. MgO is added in a molar ratio 2:1 Al/Mg (i.e., stochiometric spinel). A precipitate is formed by adding NH_4OH to maintain a pH of 8.5–9.0. The precipitate is filtered and rinsed before calcining at temperatures of up to 1,400°C. Finally, nanophase spinel aggregates are formed with a reduced (83%) density.

Even greater control of the microstructure of spinels is achieved by joint crystallization of mixtures of magnesium and aluminum salts [74, 75]. The magnesium salt, magnesium nitrate hexahydrate ($Mg(NO_3)_2{\cdot}6H_2O$) can be used to form highly reactive spinel precursors by mixing in solution with different aluminum compounds. Vasilyeva and coworkers [74, 75] for example report synthesis of nano-phase spinels with porosity of up to 50% through use of aluminum nitrate monohydrate ($Al(NO_3)_3{\cdot}9H_2O$), aluminum isopropoxide ($Al((CH_3)_2CHO)_3$), and aluminum hydroxide (AlOOH, Boehmite). The stoichiometric mixtures of salts are dissolved in water and the pH is adjusted by the addition of nitric acid (HNO_3). The solutions are evaporated and then calcined at 250–900°C. The porosity is variable and depends on the aluminum compound used, and a combustible synthesis aid such as carbon can be added to further increase the porosity.

Sol–gel techniques have also been developed to make $MgAl_2O_4$ spinel [76]. In some applications [15, 77], such as filtration membranes for the food industry, spinels, which have greater chemical stability, are prepared on the surfaces of γ-Al_2O_3 nanoparticles. In this technique, boehmite, produced by sol–gel process, is used as a starting sol. In situ modification of the sol surface is achieved by adding $Mg(NO_3)_2$ and ethylene-dinitro-tetra-acetic acid (EDTA) to the aged boehmite sol, and polyvinyl acetate (PVA) solution and polyethylene glycol (PEG) is added to prevent defect formation. During calcining, at 550–850°C, magnesium oxide diffuses to the core and reacts with the alumina to form a spinel coat on the γ-Al_2O_3 particles.

A modified sol–gel method can also be used to make spinel directly [76]. Magnesium oxide is dispersed into an isopropanol solution of aluminum sec-butoxide. Water is added to the solution to promote alkoxide gelation and the slurry is evaporated to remove excess water and alcohol. The precursors are then dried and calcined at 300–800°C. In this case the formation of spinel is through reaction of nanophase MgO and Al_2O_3 in the spinel precursor during the calcining process.

13 Lithium Aluminates

Lithium aluminates have a potentially important role in the development of new types of nuclear reactors [78–81]. This role is a result of the nuclear reaction between the ^{6}Li isotope and neutrons $^6Li(n,\alpha)$, which results in a tritium (^{3}H) ion. The natural abundance of ^{6}Li is 7.5%, so ceramics can be made without any need for isotopic enrichment. The ^{3}H ions are the plasma fuel for fusion devices. The design of the

ceramic requires a high mechanical and thermal stability so aluminates are often considered; because the operating conditions require diffusion of ^3H through pores, special synthesis conditions are required.

Lithium aluminates are also important in the development of molten carbonate fuel cells (MCFC) [82, 83]. In these fuel cells, a molten carbonate salt mixture is used as an electrolyte. These fuel cells operate through an anode reaction, which is a reaction between carbonate ions and hydrogen. A cathode reaction combines oxygen, CO_2, and electrons from the cathode to produce carbonate ions, which enter the electrolyte. These cells operate at temperatures of ~650°C and the electrolyte, which is usually lithium and potassium carbonate, is suspended in an inert matrix, which is usually a lithium aluminate.

14 Li_2O–Al_2O_3 System

As with the other aluminate systems, the binary Li_2O–Al_2O_3 is characterized by the two refractory oxide end-members, Li_2O (which melts at 1,000°C) and Al_2O_3. There are three stable compounds in the Li_2O–Al_2O_3 system: Li_5AlO_4, $LiAlO_2$, and $LiAl_5O_8$. The phases of most interest for materials application are the $LiAlO_2$ compounds that have α, β, and γ form (Fig. 3). The α-$LiAlO_2$ is orthorhombic and has the space group r3m, while the γ form has even lower (tetragonal) symmetry. Both Li and Al are in tetrahedral coordination in the γ phase. The γ phase can be produced irreversibly by sintering the α

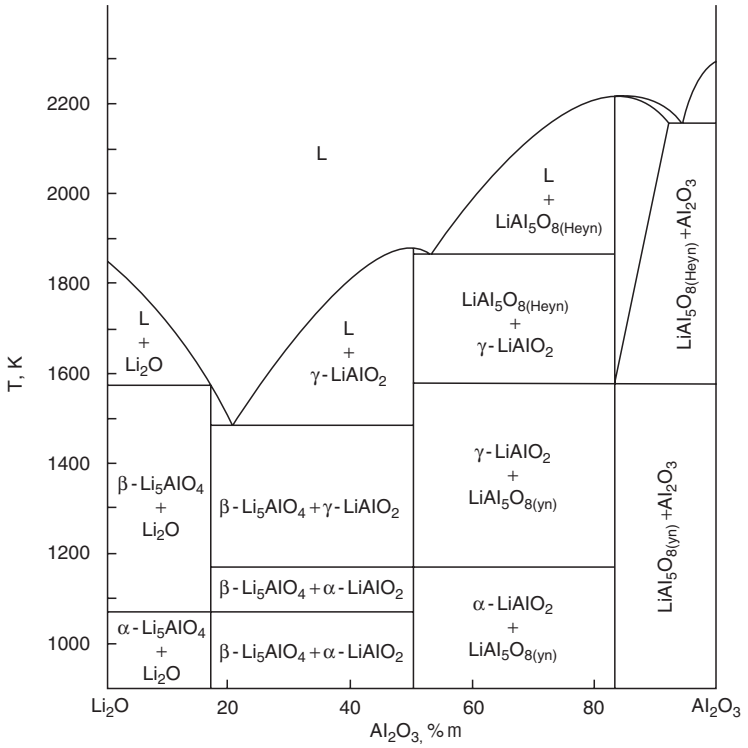

Fig. 3 The Li_2O–Al_2O_3 phase diagram [83]

phase at 1,350°C. The lattice parameters of $LiAlO_2$ match closely those of gallium nitrides, and lithium aluminates are used as a substrate for GaN epitaxial films.

15 Synthesis of Lithium Aluminates

The synthesis of lithium aluminates for tritium production requires formation of nanostructured phases. These can be made by solid-state reaction, by appropriate mixing of oxide powders [84] or by sol–gel methods [80, 85–87]. One technique is the peroxide route where γ-Al_2O_3 and $LiCO_3$ are dissolved in a peroxide (H_2O_2) solution. Evaporation of water and calcining the solid residue results in nanophase $LiAlO_2$.

Sol–gel synthesis of $LiAlO_2$ involves an alcohol–alkoxide route. Different alcohols and alkoxide combinations can be used. The alkoxide and alcohols are mixed and hydrolyzed by addition of pure water. The mixture is then gelled by heating to 60°C and is subjected to hydrothermal treatment in an autoclave. The morphology of the crystalline phases is dependent on the length of the alkoxy groups used in the alkoxide–alcohol mixing step. For example, rod-like crystals are produced with butoxide and propoxide mixtures.

16 Rare Earth Aluminates

Rare earth aluminates are extremely important as laser host materials. Most interest is in the system Y_2O_3–Al_2O_3, and of the three crystalline phases that are important in this system, the garnet phase (YAG, $Y_3Al_5O_{12}$) is the most important laser host. Laser hosts require highly transparent single crystals, and crystal growth studies of YAG were preformed at various laboratories in the 1950s and 1960s. YAG is optically isotropic and transparent from 300 nm to 4 μm and can accept trivalent laser activator ions. In 1964, the Bell Telephone Laboratories reported the lasing of YAG doped with Nd^{3+} [88]. Single crystals of YAG can be polished to form durable optical components of uniform refractive index and good thermal conductivity. Because of their robustness, YAG-based lasers have a wide variety of military, industrial, and medical applications.

Although Nd:YAG requires large, defect-free single crystals [89], polycrystalline ceramics are cheaper to manufacture and there is increasing use of YAG ceramics [90] as scintillators for radiation detection, for example Ce-doped YAG ceramics [91, 92]. In this case, the luminescence comes both from the activation of the Ce ion, with additional UV contribution, and from the YAG host itself.

Polycrystalline rare earth aluminates can also be used as advanced ceramic materials because of their refractory nature and chemical and mechanical durability. Y_2O_3–Al_2O_3 coatings are used in crystalline fibers, and Eu-doped Y-Al powders are used for phosphors and scintillation applications. Yttria and alumina are also used as additives for liquid phase synthesis of silicon nitride ceramics, often forming glassy coatings to the nitride phase and therefore having an important role in forming nitride-glass composites.

Because of the applications in laser and other optical devices, the Y_2O_3–Al_2O_3 system has been particularly well studied. There are three important crystal phases in theY_2O_3–Al_2O_3 system: in addition to the cubic garnet phase, YAG ($Y_3Al_5O_{12}$), there is a perovskite phase ($YAlO_3$) and a monoclinic phase ($Y_4Al_2O_9$). Not all rare earth aluminate binaries have a stable garnet phase. Not all rare earth aluminate systems have a stable garnet phase. The stability of the garnet phase depends on the identity of the rare earth ion [93], for larger ionic radii (e.g., La(III)), the garnet phase is not stable and only pervoskites are present.

17 Y_2O_3–Al_2O_3 System

The Y_2O_3–Al_2O_3 phase diagram [11, 94, 95] has been studied extensively [96]. Large single crystals of YAG required for laser hosts are grown from the liquid phase by the Czochralski technique and a good knowledge of the phase equilibria is required to avoid formation of phases less suited for laser and scintillation applications [11, 97, 98].

There are five crystalline compounds in the Y_2O_3–Al_2O_3 binary system (Fig. 4). The two end-members have well-known crystal structures. Y_2O_3 is cubic with two YO_6 environments and α-Al_2O_3 is trigonal with one aluminum site of AlO_6 and one oxygen site of OAl_4. The crystalline compounds show two common aluminum coordination environments (^{IV}Al and ^{VI}Al) and a range of Y–O units (YO_6, YO_7, and YO_8). There is a large range of oxygen environments. The range in coordination environments for the three ions in the Y–O–Al system have been extensively studied by nuclear magnetic resonance spectroscopy (NMR) using the ^{27}Al, ^{89}Y, and ^{17}O nuclei [99].

The garnet phase (YAG, composition $Y_3Al_5O_{12}$) has a complicated crystal structure (Fig. 5) [17, 18, 99, 100]. The garnet phase is cubic, with 160 atoms per unit cell. There are two aluminum environments in YAG: one coordinated by four oxygen atoms (^{IV}Al) and one coordinated by six oxygen atoms (^{VI}Al). There is an unique yttrium site in YAG (YO_8) and a single, distinctive oxygen environment (OY_2A_{l2}).

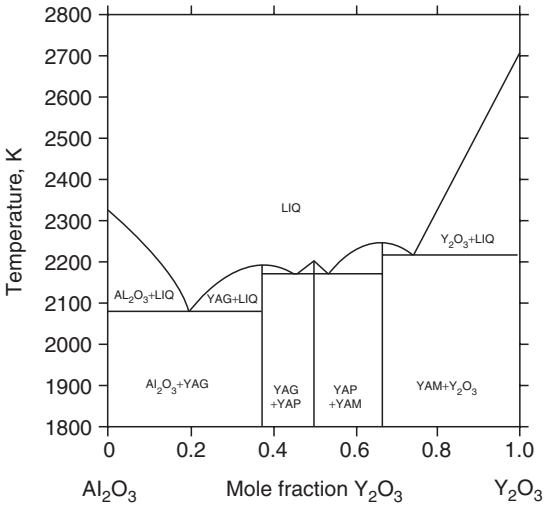

Fig. 4 The Y_2O_3–Al_2O_3 phase diagram [96–98]

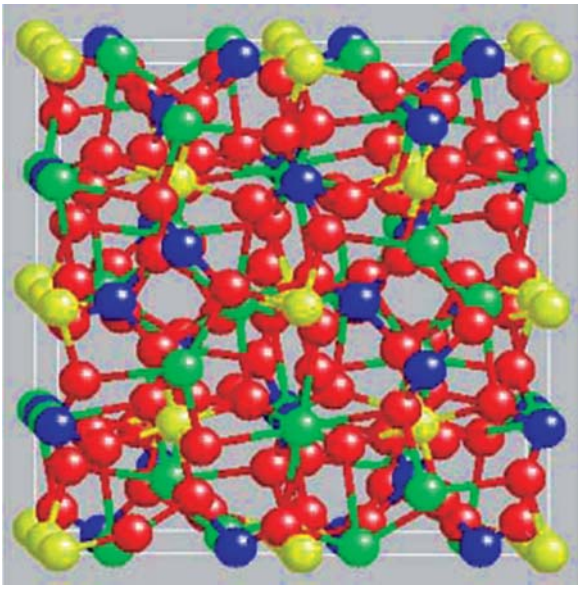

Fig. 5 The crystal structure of garnet (YAG)

The perovskite phase ($YAlO_3$) is orthorhombic and has a single type of ^{VI}Al-site (AlO_6) and a single YO_8 site. In contrast to the garnet phase, there are two oxygen sites: OY_2A_{l2} and OY_3A_{l2}. The monoclininc phase, YAM, has two different AlO_4 environments and four yttrium ions: two in YO_6 and two in YO_7. There are nine oxygen sites in YAM, four OY_3Al, two OY_2Al, two OY_4, and one OY_2A_{l2}.

Thermodynamic data from solution calorimetry using molten lead borate [95, 101] for the perovskite and garnet phases have been combined with data for the YAM phase, and heat capacity data from adiabatic calorimetry and differential scanning calorimetry have been used to calculate the phase diagram for the binary system. This recent study shows unequivocally congruent melting of the perovskite phase and that it does not decompose to the YAM phase + liquid [95].

Studies of the liquid state of Y_2O_3–Al_2O_3 liquids close to YAG have revealed complex relations in the liquid state and the existence of a metastable eutectic at 23% Y_2O_3–77% Al_2O_3 [96, 98, 102] projected form the $YAlO_3$ composition and from α-Al_2O_3. The melting temperature at this eutectic composition is 1,702°C, considerably lower than that of the melting point of YAG itself (1,940°C). The presence of this eutectic has important implications for the nucleation behavior of YAG. Under some conditions the Y_2O_3–Al_2O_3 liquids can be deeply undercooled and form a eutectic mixture of α-Al_2O_3 and YAG. This is a reflection of the difficulty in forming YAG nuclei [103], implying major differences in the local structure of the YAG-liquids and the YAG crystal phase. YAG will only form if composition are heated to a temperature of ~50°C or less above the liquid temperature [98, 104], if heated to higher temperature the liquid can be supercooled considerably below the liquid temperature and depending on conditions form a mixed ceramic or a glass (if under containerless conditions [105–107]).

Undercooled Y_2O_3–Al_2O_3 liquids are notable in that they show an unusual form of transition. This is a so-called polyamorphic transition, which is a transition from a high

density to low density amorphous phase without a change in composition [108]. This transition has been reproduced by several groups and the resultant samples comprise two glassy phases, which are amorphous. It is also to be noted that the composite samples do not consist of glass and nanocrystalline regions, as suggested by other groups [109].

18 Synthesis of YAG and Other Rare Earth Aluminates

A requirement for making YAG crystals is a homogeneous, high-purity starting material for use in the Czochralski technique. This means that the application of mechanical mixing and solid-state diffusion techniques are limited. Accordingly, a variety of synthesis techniques have been developed, most of which are sol–gel based.

The sol–gel technique is attractive because it allows for molecular mixing of constituents and results in chemical homogeneity. Typically calcining occurs at temperatures well below those required for solid-state synthesis resulting in amorphous nanocrystalline YAG samples. The citrate-based technique is commonly used for YAG synthesis [14, 110, 111]. The starting materials are aluminum and yttrium nitrates, which are soluble in water. Citric acid is added to the aqueous solution of the stoichiometric mixtures of nitrates (3:5 Y to A for YAG) to act as a chelating agent that is to stabilize the solution against hydrolysis or condensation. Ammonia is added to reduce excess acidity. The sol–gel process requires formation of an organic polymer framework, independent of the mineral species in solution. In the citrate technique, the polymer framework is based on acrylamide, which is easily soluble in water. Polymerization is initiated by free radicals and radical transfer agents. Transparent gels are obtained by heating to temperatures of ~80°C. The organic components and water are removed by placing the gel in a ventilated furnace and heating. Temperatures of 800°C result in amorphous YAG, while higher temperatures result in nanocrystalline YAG. Doping of YAG with other rare earth elements (e.g., Nd, Eu, or Tb) for phosphor or laser applications can be achieved by addition of the appropriate nitrate at the solution stage.

A translucent solution is produced by stoichiometric mixtures of aluminum isopropoxide and yttrium acetate in butanedicol and by adding glycol instead of water in the autoclave (the so-called glycothermal technique) heated to 300°C. Adding ammonium hydroxide solution causes particles of YAG to precipitate.

There are some alternatives to sol–gel based on combustion synthesis [112–114]. The motivation of combustion synthesis is similar to that for sol–gel; a homogenous high-purity product. Coprecipitation of organo-metallic products is followed by addition of a fuel, such as urea or glycerin. When heated, combustion occurs causing localized formation of YAG.

19 Y_2O_3–Al_2O_3 Glasses

Liquids in the Y_2O_3–Al_2O_3 system do not form glasses very easily, a feature that is not just coincidental with the polyamorphic transition [115–117]. Poor glass-forming ability is a feature of “fragile” liquids and the polyamorphic transition in Y_2O_3–Al_2O_3

liquids is interpreted as a transition from a fragile to strong liquid. This has important implications for materials applications of YAG and closely-related glasses.

Y_2O_3–Al_2O_3 glasses have high mechanical strength and desirable optical properties so there are potential commercial applications for YAG fibers in composite materials and optical devices. Glasses can be made from YAG using container-less levitation [13, 105, 107, 118] with fibers drawn from the beads. The lengths of the fibers are limited and this is most likely due to the changes in rheology that occur as the transition is intercepted. Furthermore, when there is formation of a second glassy phase, different properties occur leading to a "necking" and breaking of the fiber.

The unusual behavior of Y_2O_3–Al_2O_3 glasses had resulted in extensive calorimetric and diffraction studies. These suggest that the glass structure is very different from the crystalline phases [119]. Although the crystalline phases are dominated by octahedral aluminum (^{VI}Al), this short range order is reduced in the amorphous phases and the mean Al–O coordination number is close to 4 (4.15) [119]. A similar change in Y–O coordination is reported and the glass phases are not simply disordered forms of the crystalline equivalents. This observation is consistent with the fragility of Y_2O_3–Al_2O_3 liquids, and indeed molecular dynamics simulations (which are at much higher temperatures than the fictive temperatures of the glass) suggest that the Al–O coordination number increases with temperature, as further suggested by studies of levitated liquids. A structural model for a single phase (high density) Y_2O_3–Al_2O_3 glass is shown in Fig. 6.

Glasses of $Y_3Al_5O_{12}$ composition can be made by levitation techniques [106] and other glass compositions can be made at compositions close to that of the metastable eutectic (Fig. 4) using a Xe-arc image furnace. The precursors are made via sol–gel route [115].

Commercial products are being developed from single phase aluminate glasses [107, 120]. These "REAL™ Glass" materials were first made using levitation melting. Subsequently, formulations that can be cast from melts formed in platinum crucibles have been developed. The glasses are hard, strong, and environmentally stable and

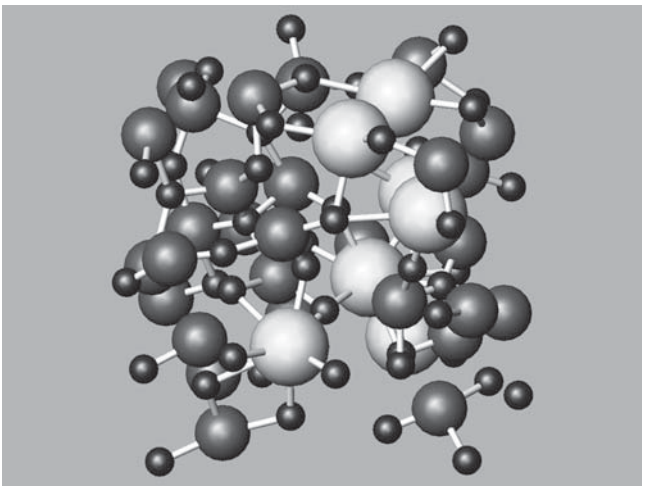

Fig. 6 Structural model of 20% Y_2O_3–80% Al_2O_3 glass

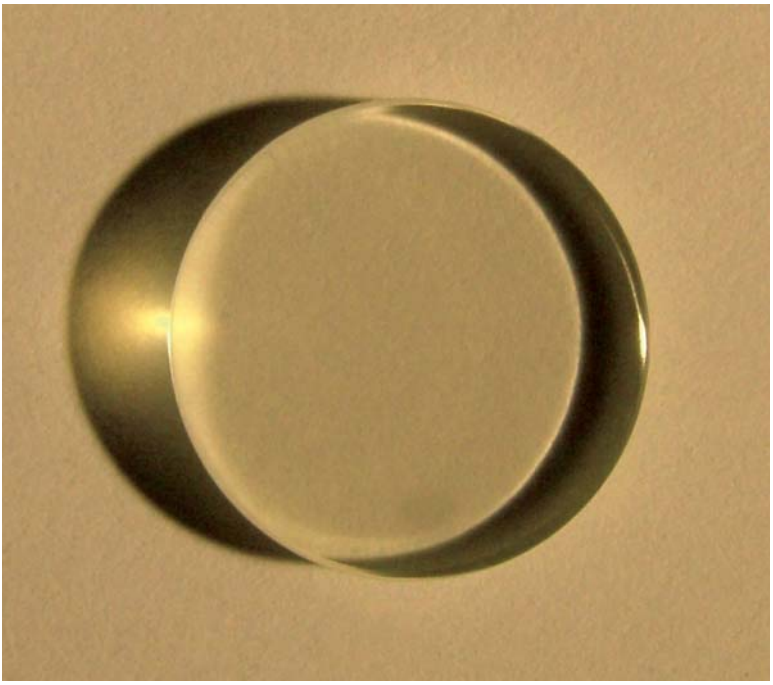

Fig. 7 A 1-cm diameter, 2-mm thick optical window made from REAL™ glass

they can be doped with high concentrations of rare earth ions for use in optical devices. Initial commercial applications are as an alternative to sapphire for use in infrared windows and optics that transmit to a wavelength of approximately 5 μm (Fig. 7). Rare earth aluminate glasses are also important medically [121]. Yttrium in rare earth aluminates can be activated by neutrons to form short-lived radioactive isotopes (^{90}Y) for cancer therapy.

20 Conclusions

Aluminate glasses and ceramics include a range of compositions and crystal structures. Most of the important physical properties of aluminates are similar to those of Al_2O_3. These properties include high melting point and high mechanical strength. Aluminate ceramics are frequently binary systems and have intermediate compounds that, while retaining the relatively high melting point, can be easily synthesized.

Aluminate compositions include calcium aluminate cements, which have high chemical resistance, especially to sulfate, and is also used in refractory applications where ordinary Portland cements would be unsuitable. These same cements are used in bioceramic applications. The bioceramic applications reflect both the high mechanical strength of the calcium aluminate cements and also the “biocompatibility” of Ca-bearing phases, which bond well with, for example, bone.

Other binary aluminates include magnesium spinels that are used extensively as castable refractory ceramics. Lithium aluminates are used, potentially, in fuel cells and as materials for new types of nuclear reactors. Again, these applications reflect the refractory nature of aluminates and their chemical resistance.

Rare earth aluminates are also important commercially as ceramics and ceramic composites for scintillation applications. The importance of the optical properties of rare earth aluminates is underscored by the used of Nd-doped YAG as a laser host.

Synthesis of aluminates is in the most part a solid-state process using purified components and requiring high temperatures. Sol–gel techniques are also used, since this is a lower temperature route and also because in many applications grain size and porosity need to be controlled.

Glasses can be formed from aluminates, but the glass-forming ability is poor. This reflects the fragility of aluminate liquids which, in Y_2O_3–Al_2O_3 systems leads to anomalous thermodynamic properties. As a result, exotic techniques are used to make aluminate glasses, most importantly container-less levitation.

Acknowledgements Dr J. K. R Weber from Materials Development Inc. kindly commented on an earlier draft of this manuscript and also provided details of the REAL™ glasses and Fig. 7. I also thank Dr. J. F. Shackelford for his support and encouragement to ensure completion of this chapter.

References

1. K.L. Scrivener, J.L. Cabiron, and R. Letourneux, High-performance concretes from calcium aluminate cements. Cement Concrete Res. **29**(8), 1215–1223 (1999).
2. K.L. Scrivener, Historical and present day applcaiitons of calcium aluminate cements, in *Calcium and Calcium Aluminate Cements*, R.J. Mangabhai and F.P. Glasser (eds.), London IOM Communications, (2001).
3. Bensted, J., High alumina cement – present state of knowledge. *Zement-Kalk-Gips*, **46**(9), 560–566 (1993).
4. Y. Liu et al., Behaviour of composite ca/p bioceramics in simulated body fluid. *Mate. Sci. Technol* **14**(6), 533–537 (1998).
5. H. Engqvist et al., Transmittance of a bioceramic dental restorative material based on calcium aluminate. *J. Biomed. Mater. Res. B-Appl. Biomater*. **69B**(1), 94–98 (2004).
6. H. Engqvist et al., Chemical and biological integration of a mouldable bioactive ceramic material capable of forming apatite in vivo in teeth. *Biomaterials*, **25**(14), 2781–2787 (2004).
7. J. Loof et al., Mechanical properties of a permanent dental restorative material based on calcium aluminate. *J. Mater. Sci.-Mater. Med.* **14**(12), 1033–1037 (2003).
8. S.H. Oh et al., Preparation of calcium aluminate cement for hard tissue repair: Effects of lithium fluoride and maleic acid on setting behavior, compressive strength, and biocompatibility. *J. Biomed. Mater. Res.* **62**(4), 593–599 (2002).
9. M.K. Cinibulk et al., Porous yttrium aluminum garnet fiber coatings for oxide composites. *J. Am. Ceram. Soc*. **85**(11), 2703–2710 (2002).
10. M.K. Cinibulk, K.A. Keller, and T.I. Mah, Effect of yttrium aluminum garnet additions on alumina-fiber-reinforced porous-alumina-matrix composites. *J. Am. Ceram. Soc.* **87**(5), 881–887 (2004).
11. L.V. Soboleva and A.P. Chirkin, Y2O3-Al2O3-Nd2O3 phase diagram and the growth of (Y,Nd)(3)Al5O12 single crystals. *Crystallog. Rep.* **48**(5), 883–887 (2003).
12. E.M. Nunes et al., A volume radiation heat transfer model for Czochralski crystal growth processes. *J. Cryst. Growth* **236**(4), 596–608 (2002).
13. J.K.R. Weber et al., Aero-acoustic levitation - a method for containerless liquid-phase processing at high temperatures. *Rev. Sci. Instrum.* **65**(2), 456–465 (1994).

14. Y.H. Zhou et al., Preparation of Y3Al5O12: Eu phosphors by citric-gel method and their luminescent properties. *Opt. Mater*. 2002. **20**(1), 13–20 (2002).
15. X.L. Pan et al., Mesoporous spinel MgAl2O4 prepared by in situ modification of boehmite sol particle surface: I Synthesis and characterization of the unsupported membranes. Colloids Surf. A-Physicochem. *Eng. Asp*. **179**(2–3), 163–169 (2001).
16. K.E. Sickafus, J.M. Wills, and N.W. Grimes, Structure of spinel. *J. Am. Ceram. Soc*. **82**(12), 3279–3292 (1999).
17. C.J. Howard, B.J. Kennedy, and B.C. Chakoumakos, Neutron powder diffraction study of rhombohedral rare-earth aluminates and the rhombohedral to cubic phase transition. *J. Phys.-Conden. Matter*. **12**(4), 349–365 (2000).
18. L. Vasylechko et al., Crystal structure of GdFeO3-type rare earth gallates and aluminates. *J. Alloys Comp*. **291**(1–2), 57–65 (1999).
19. C.E. Johnson, K. Noda, and N. Roux, Ceramic breeder materials: status and needs. *J. Nucl. Mater.* **263**(Part A) 140–148 (1998).
20. M. Poulain, Advanced glasses. *Annales de Chimie-Science des Materiaux*. **28**(2), 87–94 (2003).
21. W.A. King, and J.E. Shelby, Strontium calcium aluminate glasses. *Phys. Chem. Glasses* **37**(1), 1–3 (1996).
22. A.G. Holterhoff, Calcium aluminate cements. *Am. Ceram. Soc. Bull.* **73**(6), 90–91 (1994).
23. A.G. Holterhoff, Calcium aluminate cements. *Am. Ceram. Soc. Bull.* **74**(6), 117–118 (1995).
24. A.K. Chatterjee, An update on the binary aluminates appearing in aluminous cements, in *Calcium and Calcium Aluminate Cements*, R.J. Mangabhai and F.P. Glasser (eds.), London, IOM Communications, (2001).
25. D.A. Jerebtsov and G.G. Mikhailov, Phase diagram of CaO-Al2O3 system. *Ceram. Int*. **27**(1) 25–28 (2001).
26. B. Hallstedt, Assessment of the Cao-Al2O3 system. *J. Am. Ceram. Soc*. **73**(1), 15–23 (1990).
27. H. Pollmann, Mineralogy and crystal chemistry of calcium aluminate cement, in *Calcium and Calcium Aluminate Cements*, R.J. Mangabhai and F.P. Glasser, (eds.), London, IOM Communications (2001).
28. D.A. Brosnan and H.D. Leigh, Rehydration of castable refractories. *Can. Ceram. Q.-J. Can. Ceram. Soc*. **64**(2), 122–126 (1995).
29. W.E. Lee. et al., Castable refractory concretes. *Int. Mater. Rev* **46**(3), 145–167 (2001).
30. K. Konradsson, and J.W.V. van Dijken, Effect of a novel ceramic filling material on plaque formation and marginal gingiva. *Acta Odontol Scand*. **60**(6), 370–374 (2002).
31. S.J. Kalita, et al., Porous calcium aluminate ceramics for bone-graft applications. *J. Mater. Res.* **17**(12), 3042–3049 (2002).
32. I.N. Chakraborty, and A.K. Chattopadhyay, Manufacture of high alumina cement, an indian experience, in *Calcium and Calcium Aluminate Cements*, R.J. Mangabhai and F.P. Glasser (eds.), London, IOM Communications, 2001.
33. D.A. Fumo, M.R. Morelli, and A.M. Segadaes, Combustion synthesis of calcium aluminates. *Mater. Res. Bull*. **31**(10), 1243–1255 (1996).
34. Singh, V.K., Sintering of calcium aluminate mixes. *Br. Ceram. Trans.* **98**(4), 187–191 (1999).
35. M. Uberoi, and S.H. Risbud, Processing of Amorphous Calcium Aluminate Powders at Less-Than 900-Degrees-C. *J. Am. Ceram. Soc.* **73**(6), 1768–1770 (1990).
36. A. Varma, and A.S. Mukasyan, Combustion synthesis of advanced materials: Fundamentals and applications. Korean *J. Chem. Eng*. **21**(2), 527–536 (2004).
37. T. Aitasalo, et al., *EU2*+ doped calcium aluminates prepared by alternative low temperature routes. *Opt. Mater.* **26**(2), 113–116 (2004).
38. J.A. Sampaio, and S. Gama, EXAFS investigation of local structure of Er3+ and Yb3+ in low-silica calcium aluminate glasses - art. no. 104203. *Phys. Rev. B* **6910**(10), 4203 (2004).
39. P.F. Paradis, et al., Contactless density measurement of liquid Nd-doped 50%CaO-50%Al2O3. *J. Am. Ceram. Soc.* **86**(12), 2234–2236 (2003).
40. C.J. Benmore, et al., A neutron and x-ray diffraction study of calcium aluminate glasses. *J. Phys. Conden Matter* **15**(31), S2413–S2423 (2003).
41. M.S.F. Da Rocha, et al., Radiation-induced defects in calcium aluminate glasses. Radiat. Eff. Defects Solids **158**(1–6), 363–368 (2003).
42. W.J. Chung and J. Heo, Energy transfer process for the glue up-conversion in calcium aluminate glasses doped with Tm3+ and Nd3+. *J. Am. Ceram. Soc*. **84**(2), 348–352 (2001).

43. D.F. de Sousa et al., Energy transfer and the 2.8-mu m emission of Er3+- and Yb3+-doped low silica content calcium aluminate glasses. Phys. Rev. B **62**(5), 3176–3180 (2000).
44. W.Y. Li, and B.S. Mitchell, Nucleation and crystallization in calcium aluminate glasses. *J. Non-Cryst. Solids* **255**(2–3), 199–207 (1999).
45. P.F. McMillan, et al., A structural investigation of cao-al2o2 glasses via al-27 mas-nmr. *J. Non-Cryst. Solids* **195**(3), 261–271 (1996).
46. E.V. Uhlmann, et al., Spectroscopic properties of rare-earth-doped calcium-aluminate-based glasses. *J. Non Cryst Solids*. **178**, 15–22 (1994).
47. C.A. Angell, Glass forming liquids with microscopic to macroscopic two-state complexity. *Progress Theor. Phys. Suppl.* **126**, 1–8 (1997).
48. A.C. Hannon, and J.M. Parker, The structure of aluminate glasses by neutron diffraction. *J. Non-Cryst*. **274**(1–3), 102–109 (2000).
49. J.K.R. Weber, et al., Novel synthesis of calcium oxide-aluminum oxide glasses. *Japanese J. App. Phys. 1-Regul. Pap. Short Notes Rev Pap.* **41**(5A), 3029–3030 (2002).
50. S. Mukhopadhyay, et al., In situ spinel bonded refractory castable in relation to co-precipitation and sol-gel derived spinel forming agents. *Ceram. Int*. **29**(8), 857–868 (2003).
51. C.J. Ting, and H.Y. Lu, Hot-pressing of magnesium aluminate spinel - I. Kinetics and densification mechanism. *Acta Mater*. **47**(3), 817–830 (1999).
52. C.J. Ting, and H.Y. Lu, Hot-pressing of magnesium aluminate spinel - II. Microstructure development. *Acta Mater*. **47**(3), 831–840 (1999).
53. M.W. Vance, et al., Influence of spinel additives on high-alumina spinel castables. *Am. Ceram. Soc. Bull*. **73**(11), 70–74 (1994).
54. J.W. Lee, and J.G. Duh, High-temperature MgO-C-Al refractories-metal reactions in high-aluminum-content alloy steels. *J. Mater. Res.* **18**(8), 1950–1959 (2003).
55. A. Ghosh, et al., *Effect of spinel content on the properties of magnesia-spinel composite refractory*. *J. Eur. Ceram. Soc.* **24**(7), 2079–2085 (2004).
56. K. Goto, B.B. Argent, and W.E. Lee, Corrosion of mgo-mgal2o4 spinel refractory bricks by calcium aluminosilicate slag. *J. Am. Ceram. Soc.* **80**(2), 461–471 (1997).
57. A.H. De Aza, et al., Corrosion of a high alumina concrete with synthetic spinel addition by ladle slag. *Boletin de la Sociedad Espanola de Ceramica y Vidrio* **42**(6), 375–378 (2003).
58. B. Hallstedt, The magnesium-oxygen system. *Calphad-Comp. Coupling Phase Diagrams Thermochem*. **17**(3), 281–286 (1993).
59. B. Hallstedt, Thermodynamic assessment of the system Mgo-Al2O3. *J. Am. Ceram. Soc.* **75**(6), 1497–1507 (1992).
60. H.S.C. Oneill, and A. Navrotsky, Cation distributions and thermodynamic properties of binary spinel solid-solutions. *Am. Mineral.* **69**(7–8), 733–753 (1984).
61. F.C. Klaassen, et al., Post irradiation examination of irradiated americium oxide and uranium dioxide in magnesium aluminate spinel. *J. Nucl. Mater*. **319**, 108–117 (2003).
62. G.P. Pells, Radiation effects in ceramics. *MRS Bulle.* **22**(4), 22–28 (1997).
63. I. Ganesh, et al., An efficient MgAl2O4 spinel additive for improved slag erosion and penetration resistance of high-Al2O3 and MgO-C refractories. *Ceram. Int*. **28**(3), 245–253 (2002).
64. V.T. Gritsyna, et al., Neutron irradiation effects in magnesium-aluminate spinel doped with transition metals. *J. Nucl. Mater.* **283**(Part B), 927–931 (2000).
65. S.E. Enescu, et al., High-temperature annealing behavior of ion-implanted spinel single crystals. *J. Mater. Res.* **19**(12), 3463–3473 (2004).
66. Y.W. Lee, et al., Study on the mechanical properties and thermal conductivity of silicon carbide-, zirconia- and magnesia aluminate-based simulated inert matrix nuclear fuel materials after cyclic thermal shock. *J. Nucl. Mater.* **319**, 15–23 (2003).
67. T. Wiss, and H. Matzke, Heavy ion induced damage in MgAl2O4, an inert matrix candidate for the transmutation of minor actinides. *Radiat. Meas*. **31**(1–6), 507–514 (1999).
68. K. Yasuda, C. Kinoshita, and R. Morisaki, Role of irradiation spectrum in the microstructural evolution of magnesium aluminate spinel. *Philos. Mag. A-Phys. Condens.* Matter Struct. Defects Mechani. Properties, **78**(3), 583–598 (1998).
69. A.A. El-Kheshen, and M.F. Zawrah, Sinterability, microstructure and properties of glass/ceramic composites. *Ceram. Int.* **29**(3), 251–257 (2003).
70. A.M. Alper, et al., The system MgO-MgAl2O4. *J. Am. Ceram. Soc.* **45**(6), 263–268 (1962).
71. M. Ishimaru, et al., Atomistic structures of metastable and amorphous phases in ion-irradiated magnesium aluminate spinel. *J. Phys.-Condens. Matter* **14**(6), 1237–1247 (2002).

72. R.E. Carter, Mechanism of solid state reaction between magnesium oxide and aluminum oxide and between magnesium oxide and ferric oxide. *J. Am. Ceram. Soc.* **44**(3), 116–120 (1960).
73. H. Reveron, et al., Chemical synthesis and thermal evolution of MgAl2O4 spinel precursor prepared from industrial gibbsite and magnesia powder. *Mater. Lett.* **56**(1–2), 97–101 (2002).
74. E.A. Vasil'eva, et al., A porous ceramic based on aluminomagnesium spinel. *Russ. J. Appl. Chem.* **75**(6), 878–882 (2002).
75. E.A. Vasil'eva, et al., Specific features of the synthesis of porous materials based on a magnesium-aluminum spinel. *Glass Phys. and Chem.* **29**(5), 490–493 (2003).
76. F. Oksuzomer, et al., Preparation of MgAl2O4 by modified sol-gel method, in Euro Ceramics Viii, Parts 1–3. 2004, pp. 367–370.
77. Y.X. Pan, M.M. Wu, and Q. Su, Comparative investigation on synthesis and photoluminescence of YAG: Ce phosphor. *Mater. Sci. Eng. B-Solid State Mater. Adv. Technol.* **106**(3), 251–256 (2004).
78. L.M. Carrera, et al., Tritium recovery from nanostructured LiAlO2. *J. Nucl. Mater*. **299**(3), 242–249 (2001).
79. C.E. Johnson, K. Noda, and N. Roux, Ceramic breeder materials: status and needs. *J. Nucl. Mater.* **263**, 140–148 (1998).
80. O. Renoult, et al., Sol-gel lithium aluminate ceramics and tritium extraction mechanisms. *J. Nucl. Mater.* **219**, 233–239 (1995).
81. T. Kawagoe, et al., Surface inventory of tritium on Li2TiO3. *J. Nucl. Mater*. **297**(1), 27–34 (2001).
82. V.S. Batra, et al., Development of alpha lithium aluminate matrix for molten carbonate fuel cell. *J. Power Sources* **112**(1), 322–325 (2002).
83. K. Nakagawa, et al., Allotropic phase transformation of lithium aluminate in MCFC electrolyte plates. *Denki Kagaku* **65**(3), 231–235 (1997).
84. S. Sokolov, and A. Stein, Preparation and characterization of macroporous gamma-LiAlO2. *Mater. Lett*. **57**(22–23), 3593–3597 (2003).
85. M.A. Valenzuela, et al., Solvent effect on the sol-gel synthesis of lithium aluminate. *Mate. Lett.* **47**(4–5), 252–257 (2001).
86. M.A. Valenzuela, et al., Sol-gel synthesis of lithium aluminate. *J. Am. Ceram. Soc.* **79**(2), 455–460 (1996).
87. F. Oksuzomer, et al., Effect of solvents on the preparation of lithium aluminate by sol-gel method. *Mater. Res. Bulle*. **39**(4–5), 715–724 (2004).
88. J.E. Geusic, H.M. Marcos, and V.U. L.G., Laser oscillations in Nd-doped yttrium aluminum, yttrium gallium, and gadolinium garnets. *App. Phys. Lett*. **4**, 182–184 (1964).
89. E. Zych, C. Brecher, and J. Glodo, Kinetics of cerium emission in a YAG: Ce single crystal: the role of traps. *J. Phys. Condens. Matter.* **12**(8), 1947–1958 (2000).
90. J.R. Lu, et al., Neodymium doped yttrium aluminum garnet (Y3Al5O12) nanocrystalline ceramics – a new generation of solid state laser and optical materials. *J. Alloys Compd*. **341**(1–2), 220–225 (2002).
91. E. Zych, and C. Brecher, Temperature dependence of Ce-emission kinetics in YAG: Ce optical ceramic. *J. Alloys Compd.* **300**, 495–499 (2000).
92. E. Zych, et al., Luminescence properties of ce-activated yag optical ceramic scintillator materials. *J. Luminescence* **75**(3), 193–203 (1997).
93. Y. Kanke, and A. Navrotsky, A calorimetric study of the lanthanide aluminum oxides and the lanthanide gallium oxides: stability of the perovskites and the garnets. *J. Solid State Chem.* **141**(2), 424–436 (1998).
94. M. Medraj, et al., High temperature neutron diffraction study of the Al2O3-Y2O3 system. *J. Eur. Ceram. Soc*. **26**(16), 3515–3524 (2006).
95. O. Fabrichnaya, et al., The assessment of thermodynamic parameters in the Al2O3-Y2O3 system and phase relations in the Y-Al-O system. Scand. *J. Metall*. **30**(3), 175–183 (2001).
96. J.L. Caslavsky, and D. Viechnicki, Phase-equilibria studies in the ternary-system Al2O3/Y2O3/Nd2O3 using odta. *Am. Ceram. Soc. Bulle.* **61**(8), 808–808 (1982).
97. J.L. Caslavsky, and D. Viechnicki, Melt Growth of Nd - Y3al5o12 (Nd-Yag) Using the Heat-Exchange Method (Hem). *J. Cryst. Growth*. **46**(5), 601–606 (1979).
98. J.L. Caslavsky, and D.J. Viechnicki, Melting behavior and metastability of yttrium aluminum garnet (Yag) and YAlO3 determined by optical differential thermal-analysis. *J. Mater. Sci.* **15**(7), 1709–1718 (1980).
99. P. Florian et al., A multi-nuclear multiple-field nuclear magnetic resonance study of the Y2O3-Al2O3 phase diagram. *J. Phys. Chem.* B. **105**(2), 379–391 (2001).

100. I. Zvereva et al., Complex aluminates RE2SrAl2O7 (RE = La, Nd, Sm-Ho): Cation ordering and stability of the double perovskite slab-rocksalt layer P-2/RS intergrowth. Solid State Sci. **5**(2), 343–349 (2003).
101. O. Fabrichnaya et al., Phase equilibria and thermodynamics in the Y2O3-Al2O3-SO2-system. *Zeitschrift fur Metallkunde* **92**(9), 1083–1097 (2001).
102. B. Cockayne, and B. Lent, A complexity in the solidification behavior of molten Y3Al5O12. *J. Cryst. Growth*. **46**, 371–378 (1979).
103. B.R. Johnson, and W.M. Kriven, Crystallization kinetics of yttrium aluminum garnet (Y3Al5O12). *J. Mater. Res.* **16**(6), 1795–1805 (2001).
104. M. Gervais et al., Crystallization of y3al5o12 garnet from deep undercooled melt effect of the al-ga substitution. *Mater. Sci. Eng. B-Solid State Mater. Adv. Technol.* **45**(1–3), 108–113 (1997).
105. J.K.R. Weber et al., Growth and crystallization of YAG- and mullite-composition glass fibers. *J. Eur. Ceram. Soc.* **19**(13–14), 2543–2550 (1999).
106. J.K.R. Weber et al., Structure of liquid Y3Al5O12 (YAG). *Phys. Rev. Lett.* **84**(16), 3622–3625 (2000).
107. J.K.R. Weber et al., Glass formation and polyamorphism in rare-earth oxide-aluminum oxide compositions. *J. Am. Ceram. Soc.* **83**(8), 1868–1872 (2000).
108. S. Aasland, and P.F. McMillan, Density-driven liquid-liquid phase separation in the system al2o3-y2o3. *Nature* **369**(6482), 633–636 (1994).
109. K. Nagashio, and K. Kuribayashi, Spherical yttrium aluminum garnet embedded in a glass matrix. *J. Am. Ceram. Soc.* **85**(9), 2353–2358 (2002).
110. A. Douy, Polyacrylamide gel: an efficient tool for easy synthesis of multicomponent oxide precursors of ceramics and glasses. *Int. J. Inorg. Mater.* **3**(7), 699–707 (2001).
111. J.J. Zhang et al., Low-temperature synthesis of single-phase nanocrystalline YAG: Eu phosphor. *J. Mater. Sci. Lett.* **22**(1), 13–14 (2003).
112. J. Marchal et al., Yttrium aluminum garnet nanopowders produced by liquid-feed flame spray pyrolysis (LF-FSP) of metalloorganic precursors. *Chem. Mater.* **16**(5), 822–831 (2004).
113. S.D. Parukuttyamma et al., Yttrium aluminum garnet (YAG) films through a precursor plasma spraying technique. *J. Am. Ceram. Soc.* **84**(8), 1906–1908 (2001).
114. S. Ramanthan et al., Processing and characterization of combustion synthesized YAG powders. *Ceram. Int.* **29**(5), 477–484 (2003).
115. M.C. Wilding, and P.F. McMillan, Polyamorphic transitions in yttria-alumina liquids. *J. Non Cryst. Solids* **293**, 357–365 (2001).
116. M.C. Wilding, P.F. McMillan, and A. Navrotsky, Calorimetric study of glasses and liquids in the polyamorphic system Y2O3-Al2O3. *Phys. Chem. Glasses* **43**(6), 306–312 (2003).
117. M.C. Wilding, P.F. McMillan, and A. Navrotsky, Thermodynamic and structural aspects of the polyamorphic transition in yttrium and other rare-earth aluminate liquids. *Phys. Stat. Mech. Appl.* **314**(1–4), 379–390 (2002).
118. J.K.R. Weber et al., Glass fibres of pure and erkium- or neodymium-doped yttria-alumina compositions. *Nature* **393**(6687), 769–771 (1998).
119. M.C. Wilding, C.J. Benmore, and P.F. McMillan, A neutron diffraction study of yttrium- and lanthanum-aluminate glasses. *J. Non-Cryst. Solids* **297**(2–3), 143–155 (2002).
120. J.K.R. Weber, US patent 6,482,758; Single phase rare earth oxide aluminum oxide glasses. 2002: US.
121. T.E. Day, and D.E. Day, Manufacturing RadSpheres. *Am. Ceram. Soc. Bull.* **83**(8), 21–21 (2004).